Iranian Journal of Pharmaceutical Sciences
Summer 2008: 4(3): 201-208
www.ijps.ir

Original Article

The Effect of Rotation Speed and Time of Milling on Synthesis and Properties of Fluoridated Hydroxyapatite Biomaterial

Mohammad Hossein Fathi*, Ehsan Mohammad Zahrani

Biomaterials Group, Materials Engineering Department, Isfahan University of Technology, Isfahan, Iran

Abstract

Synthetic hydroxyapatite (HA) is the most helpful because of its similarity to natural bone in both crystalline structure and chemical composition. Recently, fluoridated hydroxyapatite (FHA) has been developed in dental and orthopedic application because it has lower solubility than pure HA, while maintaining the comparable bioactivity and biocompatibility. The aim of this study was to synthesis and characterizes FHA nanopowder via mechanochemical activation method. Also the effect of milling time and rotation speed on its properties was investigated. Calcium hydroxide, phosphorous oxide and calcium fluoride powder were used for synthesis of FHA. The math ratio of balls to reactant was 30. Mechanochemical reaction was performed in the planetary ball mill at two rotating speed 300 and 250 rpm. Zirconia ball and zirconia vial were used to perform the mechanochemical process. X-ray Diffraction, FTIR spectroscopy and Scanning Electron Microscopy were utilized to characterize FHA nanopowder. The results showed that the synthesis of FHA after 6 h ball milling at 300 rpm or 10 h milling at 250 rpm was complet.

Keywords: Crystallite size; Fluoridated hydroxyapatite; Mechanochemical activation; Milling time; Nanopowder; Rotation speed.
Received: December 4, 2007; *Accepted:* March 27; 2008

1.Introduction

Tissue diseases and defects, particularly bone diseases are serious health condition that directly affects the quality of life of the sufferers. Within the last four decades, innovative use of specially designed ceramics for the repair and reconstruction of diseased or damaged parts of the body has revolutionized the treatment methods [1]. Ceramics used for this purpose are termed bioceramics. Replacement of tissues has two alternatives: (1) transplantation and (2) implantation. The significant advantages of bioceramics as implants over transplants are availability, reproducibility and reliability. Moreover, they do not pose the risk of any viral or bacterial infection to patients [2, 3].

Apatites like hydroxyapatite (HA) are very important inorganic biomaterials. They have good bioactivity and osteoconducivity, and are used as bulk ceramics, coatings and granules in clinical applications. HA which is

*Corresponding author: Mohammad Hossein Fathi, Biomaterials Group, Materials Engineering Department, Isfahan University of Technology, 84156 Isfahan, Iran.
Fax (+98)311-3912752, Tel (+98)311-3915708.
E-mail: Fathi@cc.iut.ac.ir

represented by the formula $Ca_{10}(PO_4)_6(OH)_2$ is one of the inorganic components of the hard tissues of living bodies such as bones, teeth, etc [3]. HA is a calcium phosphate-based bioceramic which has been used in medicine and dentistry for over 20 years because of its excellent biocompatibility with human tissues. Thus, HA has been widely used in dental implants, alveolar bridge augmentation, orthopedics, maxillofacial surgery, etc [3].

Fluorine as a micro-element is necessary for the normal dental and bone formation in body. Fluorine ions can promote apatite formation and optimize the solubility of apatites [4]. When a small amount of fluorine is present in apatite as a fluoroapatite (FA)/fluorohydroxyapatite (FHA) solid solution, the crystalline of the apatite increases and the solubility decreases greatly [4, 5]. FHA has been increasingly investigated as clinical restoration materials for stimulatory purpose in hard tissues or for maintaining the stability of materials during processing. It was reported that FHA could provide sufficient low levels of fluoride to affect the surrounding cells for improving bone formation, while avoiding unnecessary accumulation within the body [6].

Pure FA has a lower bio-resorption rate than HA, and has a level of biocompatibility comparable to that of HA, demonstrating properties such as fixation to bone and bone ingrowths [7, 8]. Moreover, FA forms a FHA $[Ca_{10}(PO_4)_6(OHF)_2]$ solid solution with HA by replacing F- with OH- over a wide range of concentrations [9]. In practice, F- itself has been widely investigated in dental restoration areas, because it prevents dental cavies in a bacteria containing, acidic environment [10, 11]. Furthermore, F- promotes the mineralization and crystallization of calcium phosphate in the bone forming process [12].

Thus, the synthesis of FHA is of great value and has been widely investigated by multiple techniques, such as precipitation, sol-gel, hydrolysis, hydrothermal, emulsion processing routes, etc. However most of these methods need precise controls on the processing condition and the composition and properties of final products are strongly influenced by various parameters [13, 14]. The procedure and the apparatus for these processes are complicated and are not suitable for mass production [15].

Mechanochemical powder synthesis is a solid-state synthesis method that takes advantage of the perturbation of surface-bonded species by pressure to enhance

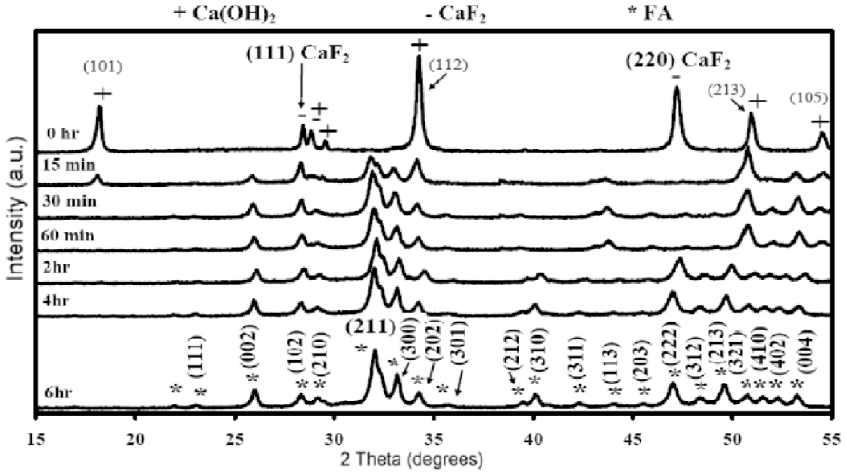

Figure 1. XRD-pattern of untreated and mechanochemically treated mixture of Ca $(OH)_2$-P_2O_5- CaF_2.

thermodynamic and kinetic reactions between solids [16]. In many cases, mechanochemistry can be used to prepare anhydrous multi-component oxides at room temperature in a single step. Pressure can be applied via conventional milling equipment ranging from low-energy ball mills to high energy stirred mills (e.g. attrition, planetary, or vibratory mills). The main advantages of mechano-chemical synthesis of ceramic powders are simplicity and low cost.

However, little attention has been paid to the synthesis of such biologically interesting FHA powders via this simple method. Thus the object of present work was synthesis and characterization of FHA nanopowder by mechanochemical activation.

2. Materials and methods

2.1. Synthesis of FHA nanopowder

Calcium hydroxide, phosphorous oxide and calcium fluoride powders, used for synthesis of FHA, were purchased from Merck. The appropriate amounts of starting materials were mixed. The mole ratio of calcium hydroxide to phosphorous oxide and calcium fluoride was 9:3:1. The math ratio of balls to reactant was 30, whereby the overall ball mass was 175 g. Mechanochemical reaction was performed in a planetary ball (FRETCH) mill at the two rotating speed 300 and 250 rpm. Zirconia ball and zirconia vial were used to perform the mechanochemical process. Eight balls with 2 cm diameter were utilized. Ball milling time varied from 0 to 10 h.

2.2. X-ray diffraction analysis

The powders obtained were identified in an X-ray diffract meter (XRD, Philips Xpert) using Nickel filtered CuKα ($\lambda_{CuK\alpha}$=0.154186 nm) radiation at 40 kV and 100 mA. Time per step 2.5 and step size of 0.02° were selected over the 2θ range of 15-55°. The experimental patterns obtained were compared to standards compiled by the Joint Committee on Powder Diffraction and Standards (JCPDS), which involved card # 09-0432 for HA, # 15-0876 for FA, # 35-0816 for CaF_2 ,# 04-0733 for $Ca(OH)_2$,# 25-0254 for $CaZrO_3$ and # 27-0997 for ZrO_2 .

2.3. Determination of the size of nanoparticles

The FA crystallite size and lattice strain was estimated with broadening of XRD peaks by Williamson-Hall formula [17] as the following:

$$B\cos\theta = \frac{0.89\,\lambda}{d} + \eta\sin(\theta)$$

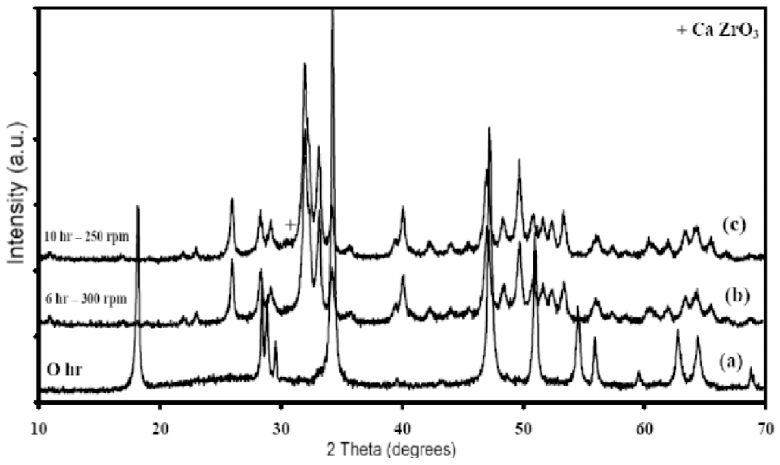

Figure 2. XRD-pattern of mixture $Ca(OH)_2$-P_2O_5- CaF2 mechanochemically treated for (a) 0 h, (b) 6 h at 300 rpm and (c) 10 h at 250 rpm.

where λ is the wavelength of the X-ray tube, B is width of peak in the middle of its height that was measured with Sigma-plot software and θ is Bragg's angle. Thus, when BCos(θ) is plotted against sin(θ), a straight line is obtained with the slope as η and the intercept as 0.89λ/d. From these, one can calculate the crystallite size d and the lattice strain η, (002), (112) and (222) peaks of FA was used in this techniques.

2.4. FT-IR Spectroscopy

Infrared spectra of the prepared powder were obtained in the range of 400-4000 cm^{-1} using a Fourier-transform infrared spectrometer (FT-IR, Bomem, MB 100). For this purpose each powder was mixed with KBr in the proportion 1/100 (by weight) for 15 min., and pressed into a pellet using a hand press. The FT-IR spectra were acquired with resolution of 4.0 cm^{-1}.

2.5. Scanning electron microscopy (SEM)

The morphology and the agglomerate size distribution of the milled powders were studied by SEM (Phillips XL 30).

3. Result and discussion

Figure 1 shows the XRD patterns of $Ca(OH)_2$-P_2O_5-CaF_2 powder mixture, mechanically alloyed for 15 min. to 6 h. An XRD pattern of mixture before milling is given in the same figure for comparison.

At the beginning, only sharp characteristic peak of $Ca(OH)_2$ and CaF_2 were observed. Characteristic peak of P_2O_5 was not observed at the powder mixture before milling because P_2O_5 had low crystalline and its peaks disappears in the background of XRD pattern. With the prolonged milling, these sharp peaks of starting materials degraded significantly. The X-ray pattern of the sample, milled for 2 h, shows the most intense peaks for $Ca(OH)_2$ [(101) at 2θ = 18.25°, (112) at 2θ = 34.2° , (213) at 2θ = 51.05°], while the most intense peaks for CaF_2 [(111) at 2θ = 28.2°; (220) at 2θ = 47.1°] disappeared at the first time of milling. The X-ray pattern of the samples milled for 15min. - 4 h confirm continuation of mechanochemical process. When the milling duration was increased to 15 min., the emergence of the peak around 31.7° indicated the formation of apatite. Further increase in milling time up to 6 h resulted in further increase in crystalline order of the FA phase - further sharpening of the principal diffraction peaks (Figure 1). However, the broad envelope shape of FA peaks at the first times of milling revealed that newly formed apatite

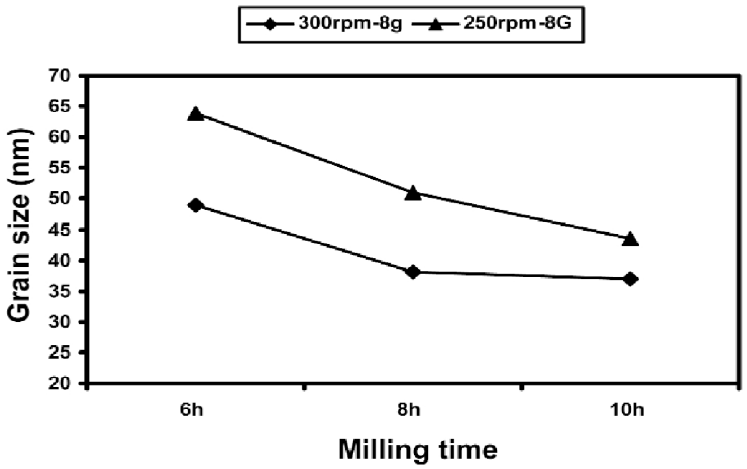

Figure 3. Effect of rotation speed and milling time on crystallite size of milled powder.

was poorly crystallized after 15 min. milling. The peaks of the starting powders gradually became weaker, but the decreasing rate of each starting material differed. By comparing the relative intensities of CaF_2, (111) and (220) peaks at $2\theta = 28.2°$ and $2\theta = 47.1°$ and $Ca(OH)_2$, (101), (112) and (213) peaks at $2\theta = 18.25°$, $2\theta = 34.2°$ and $2\theta = 51.05°$, it was found that peak intensity of $Ca(OH)_2$ decreased relative slowly. After milling for 15 min. CaF_2 completely vanished, but the XRD pattern showed the considerable amount of calcium hydroxide remained. Since the starting materials were mixed according to the stoichiometric ratio and the XRD traces from 15 min. to 1 h showed that there were only two identified phases, apatite and calcium hydroxide. After milling for 6 h, the relatively well-crystalline FA, as evidenced by the splitting of peaks around 31-35°, had the matched relative intensity with the standard card of FA (JCDP # 15-0876), specially at 28.2°, where the peak of apatite (102) plane was often overlapped by CaF_2 (111) indicating any remained CaF_2. The diminution of diffraction peaks of calcium fluorides further served as the evidence that fluoride ions entered into the crystal structure of apatite and formed fluoroapatite.

XRD-patterns of mixture of $Ca(OH)_2$, P_2O_5, CaF_2 - mechanochemically treated for 6 h at 300 rpm and 10 h at 250 rpm - was compared with XRD-patterns of the mixture before milling in Figure 2. The comparison between these three patterns indicated the FA synthesis after 6 h milling at 300 rpm or after 10 h milling at 250 rpm. Sharpness of peaks showed high crystalline order of FA. But after 10 h milling at 250 rpm $CaZrO_3$ identified as an impurity in prepared FA powder.

When OH^- ions are substitute with F^- there is more distortion in the structure because of the larger ionic radii of F^-. At the end of process, the F^- ion occupies a larger space in the center of the lattice, thus forming stable FA structure.

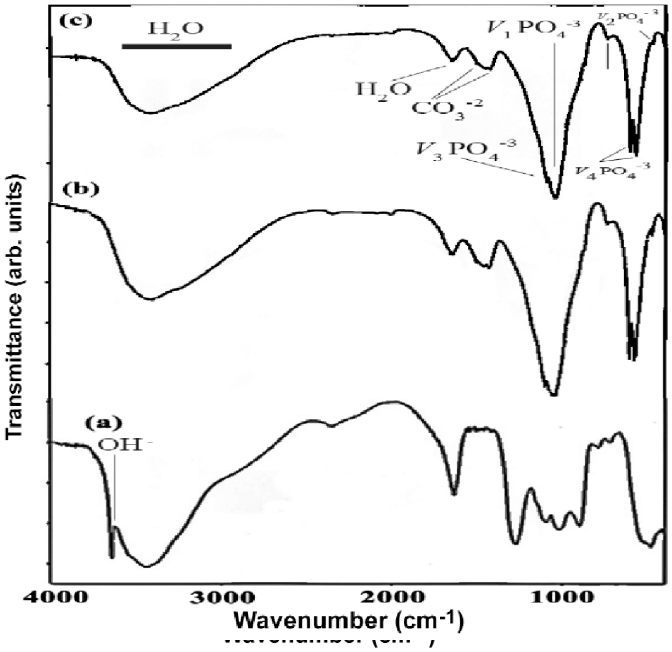

Figure 4. The FT-IR spectrum of the mixture of $Ca(OH)_2$-P_2O_5 - CaF_2 after (a) 0 h, (b) 6 h at 300 rpm and (c) 10 h at 250 rpm.

The crystallite size for the sample milled for 6, 8 and 10 h was calculated with broadening of XRD peaks by Williamson-Hall formula [17] and is given in Figure 3. Prolonged milling caused a decrease in crystallite size. Results showed that crystallite size decreased with decreasing in rotation speed. Also after 8 h milling, crystallite size decreased more slowly.

In Figure 4, FT-IR spectra of the sample milled for 6 h at 300 rpm and 10 h at 250 rpm was compared with FT-IR spectra of initial powder mixture. The band at 474 cm^{-1} corresponds to the asymmetrical υ_2 stretching vibration, the band at 574 and 603 cm^{-1} corresponds to the asymmetrical υ_4 stretching vibration, the band at 1044 and 1095 cm^{-1} correspond to the asymmetrical υ_3 stretching vibration, and bands at 965 correspond to the asymmetrical υ_1 stretching vibration of the phosphate group (PO_4^{3-}) [18,19,20]. The band at 1651 cm^{-1} corresponds to the bending vibration of the hydroxyl (OH^-) group in H_2O molecules. A double bond appears at 1430 and 1457 cm^{-1} that corresponds to υ_3 vibrations of the carbonate group (CO_3^{2-}). The band at 736 cm^{-1} corresponds to the shifting OH^- liberation mode. This is caused by the increase of F^- content in the (OH^-, F^-) chain of apatite with predominant configuration of ...FHO: OHF... [20].

According to the literature [15] the (OH^-, F^-) chain of apatite should contain at least three types of [OH^-] and a possibly one of these four distinguishable vibration energies: (1) the "normal" [OH^-] in an extended [OH^-] chain (configuration ...OHOHOH...). (2) "Tail to tail" configuration HO: OH, (3) the F^- bonded [OH^-] in the symmetrical configuration ...OHFHO..., (4) in F^- rich chains containing only a few [OH^-], in which the F^- bonded [OH^-] has an asymmetrical configuration ...FFOHFF....

In general H, F apatite chains have ...FHO (OH)-nHO:OH(OH)-nOHF... configuration where n depends on OH^- and F^- ratio within the apatite. The number of n decreases with increasing F^- ion content, and there is a ...FHOHO:OHOHF... configuration for n=0. With further increase of F- *vs*. OH- ion content in apatite, the number of OH- ions reduces in the chain until the formation of FHO:OHF and ...FOHF... chain configuration is reached.

In Figure 5, morphology and size distribution of the agglomerates/particles was showed. No significant changes in size distribution and morphology of the agglomerates / particles can be observed for the samples milled for 6 h at 300 rpm and 10 h at 250 rpm. This is especially valid for the largest particles. Only accumulated fine particles and lamina of polygonal shape are visible on the surfaces of larger particles. As it is shown in Figure 4, agglomerates of all

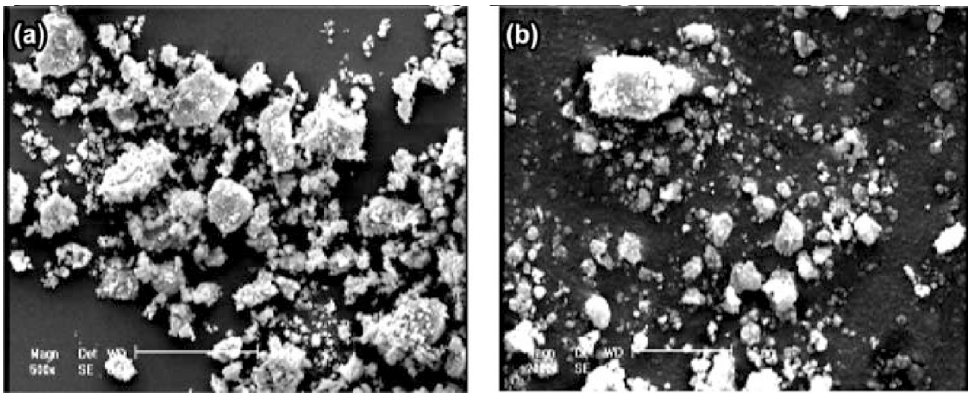

Figure 5. SEM micrograph of the samples milled for: (a) 6 h at 300 rpm and (b) 10 h at 250 rpm.

samples are sized from 10- 45 μm. Fine agglomerates consist of significantly finer agglomerates/particles that cannot be seen individually in microphotographs because of their particular small size. Very fine accumulated particles 2-9 μm in size. In addition, the micrographs give us an idea about fine agglomerates of particles interconnected, in different ways, into structures of different forms, morphology and distribution. No significant differences in the particle size distribution can be observed in microphotographs of the milled samples.

4. Conclusion

Fluorine apatite was successfully synthesized from $Ca(OH)_2$, P_2O_5 and CaF_2 via a mechanochemical activation method. X-ray diffraction and FT-IR was used to identify the resulted powder as FA nanocrystals with the crystallite size of 49 nm after 6 h milling at 300 rpm and 43 nm after 10 h milling at 250 rpm. However, after 10 h milling at 250 rpm $CaZrO_3$ identified as an impurity in prepared FA powder. The appearance of a band at 736 cm^{-1} that confirms complete exchange OH^- with F^-.

Calculation of crystallite size in difference milling time and rotation speed showed that crystallite size of samples decreased with increasing rotation speed of ball mill and with increasing of milling time the rate of decreasing crystallite size was more lower. It can be concluded that the mechanochemical synthesis depends mainly on the rate of particle deformation and the velocity of impact waves.

References

[1] Hench LL. Bioceramics: From concept to clinic. *J Am Ceram Soc* 1991, 74: 1487-510.

[2] Hench LL, Wilson J. *Introduction to bioceramics*. Singapore: World Scientific, 1993.

[3] Ranter BD, Hoffman AS, Schoen FJ, Lemons JE. *Biomaterials science. An introduction to materials in medicine*. San Diego: Academic Press, 1996; p. 484.

[4] Amjad Z. *Calcium phosphates in biological and industrial systems*. Boston: Kluwer Academic Publishers, 1998; pp. 67-83.

[5] Vaughan J. *The physiology of bone*. Oxford: Clarendon Press, 1981; p. 96.

[6] Gross KA, Rodri´guez-Lorenzo LM. Mechanochemical hydrothermal synthesis and characterization of fluoridated hydroxyapatite, *Biomaterials* 2004; 25: 1385.

[7] Overgaard S, Lind M, Grundvig H, Biinger C, Soballe K. Hydroxyapatite and fluorapatite coatings for fixation of weight loaded implants. *Clin Orthop Rel Res* 1997; 336: 286-96.

[8] Slosarczyk A, Stobierska E, Paszkiewicz Z, Gawlick M. Calcium phosphate materials prepared from precipitates with various calcium: Phosphorus molar ratios. *J Am Ceram Soc* 1996; 79: 2539-44.

[9] Posner AS. The mineral of bone. *Clin Orthop* 1985; 200: 87-99.

[10] Moreno EC, Kresak M, Zahradnik RT. Fluoridated hydroxyapatite solubility and caries formation. *Nature* 1974; 247: 64-5.

[11] Legeros RZ, Silverstone LM, Daculsi G, Kerebel LM. *In vitro* caries-like lesion formation in F-containing tooth enamel. *J Dent Res* 1985; 62: 138-44.

[12] Kim W, Zhang QW, Saito F. Mechanochemical synthesis of hydroxyapatite from $Ca(OH)_2$-P_2O_5 and $Ca(OH)_2$-P_2O_5 mixtures. *J Mater Sci* 2000; 35: 5401-5.

[13] Rodri´guez-Lorenzo LM, Hart JN, Gross KA. Influence of fluorine in the synthesis of apatites. Synthesis of solid solutions of hydroxy-fluotapatite. *Biomaterials* 2003; 24: 3777-85.

[14] Suchanek WL, Yoshimura M. Processing and properties of hydroxyapatite-based biomaterials for use as hard tissue replacement implants. *J Mater Res* 1998; 13: 94-117.

[15] Rhee SH. Synthesis of hydroxyapatite via mechanochemical treatment. *Biomaterials* 2002, 23: 1147.

[16] Gutman E. *Mechanochemistry of Materials*. Cambridge: International Science Publishing, 1997.

[17] Williamson K, Hall WH. X-ray line broadening from filed aluminium. *Acta Metall* 1953; 1: 22-31.

[18] Nikcevic I, Jokanovic V, Mitric M, Nedic Z, Makovec D, and Uskokovic D. Mechanochemical synthesis of nanostructured fluorapatite/fluorhydroxyapatite and carbonated fluorapatite/fluorhydroxyapatite. *J Solid State Chem* 2004; 177: 2565-74.

[19] Nyquist RA, Kagel RO. *Infrared spectra of inorganic compounds*. New York: Academic

Press, 1971; p. 493.
[20] Nakamoto K. *Infrared and Raman spectra of inorganic and coordination compounds*. New York: Wiley, 1978.